

Orientation Cutting of TlBr Crystals via Pole Figure Measurements for Gamma-Ray Detector Fabrication

Toshiyuki Onodera¹, Mitsuhiro Nogami², Keitaro Hitomi² and Hidenori Toyokawa³

Tohoku Institute of Technology¹, JAPAN, Tohoku University², JAPAN and Konan University, JAPAN

t_onodera@tohtech.ac.jp

Introduction

Thallium Bromide (TlBr) semiconductor

Atomic number Tl: 81, Br: 35	High detection efficiency
Density 7.56 g/cm ³	
Band-gap energy 2.68 eV	Room temperature operation
$\mu_e \tau_e \sim 10^{-3} \text{ cm}^2/\text{V}$	High energy resolution
$\mu_h \tau_h \sim 10^{-4} \text{ cm}^2/\text{V}$	
Melting point 460 °C	Easy to grow
Phase transition No	

→ Promising material for gamma-ray detectors

Gamma-ray imaging using TlBr

Prototype TlBr imaging detector

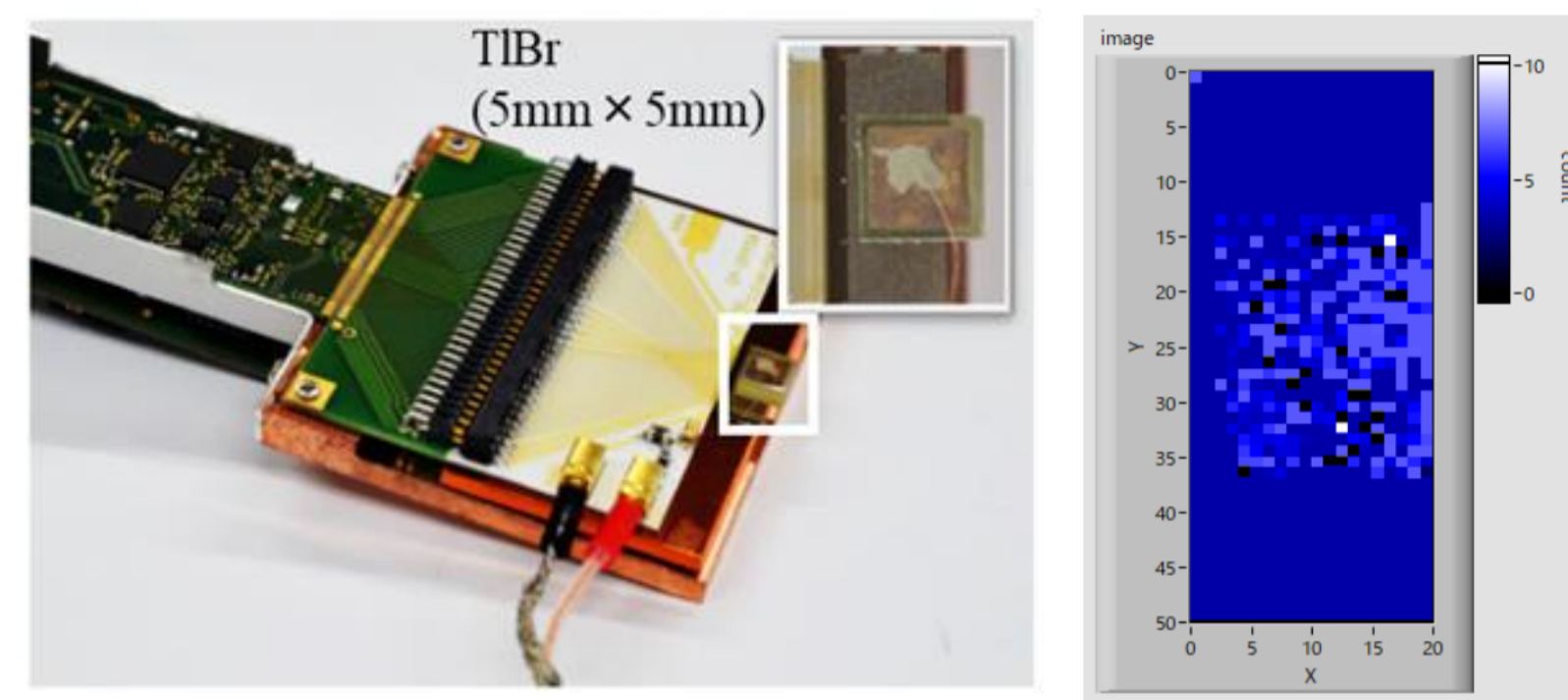
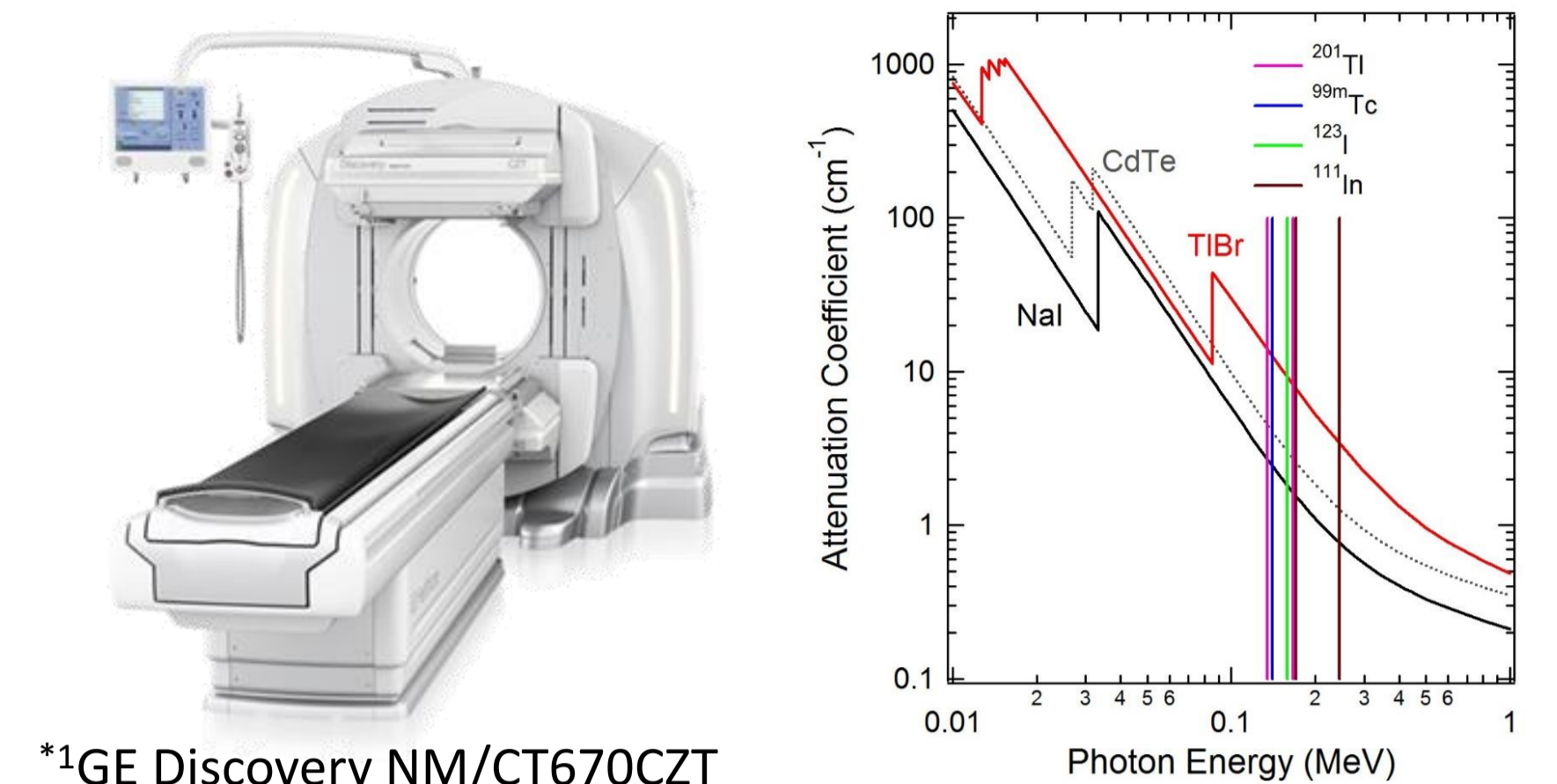


Fig. 1. Prototype of 2 dimensional imaging detector using a TlBr crystal (5 mm x 5 mm) and obtained image by ¹³⁷Cs gamma-ray irradiation at JASRI.

Future applications in medical imaging



*1: GE Healthcare
Fig. 2. Linear attenuation coefficient for TlBr and typical detector materials (NaI, CdTe), and gamma-rays energy used in SPECT diagnosis.

Challenges in TlBr detector fabrication

Dependence of detector performance on TlBr crystal orientation remains unresolved.

In this study, we aimed to establish a technique for slicing TlBr wafers with specified crystallographic orientations from ingots, using pole figure measurements, and to evaluate detector performance for each orientation.

- Experiment 1: Crystallographic characterization by pole figure measurements
- Experiment 2: Slicing TlBr wafers with (100), (111), and (110) orientations.

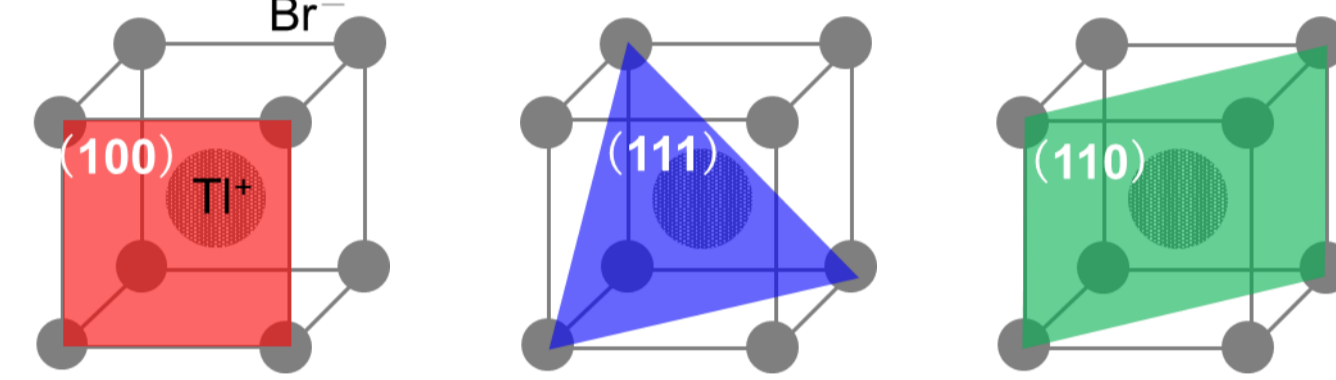


Fig. 3. Crystal structure of TlBr.

Exp.1: Pole figure measurements

TlBr crystal

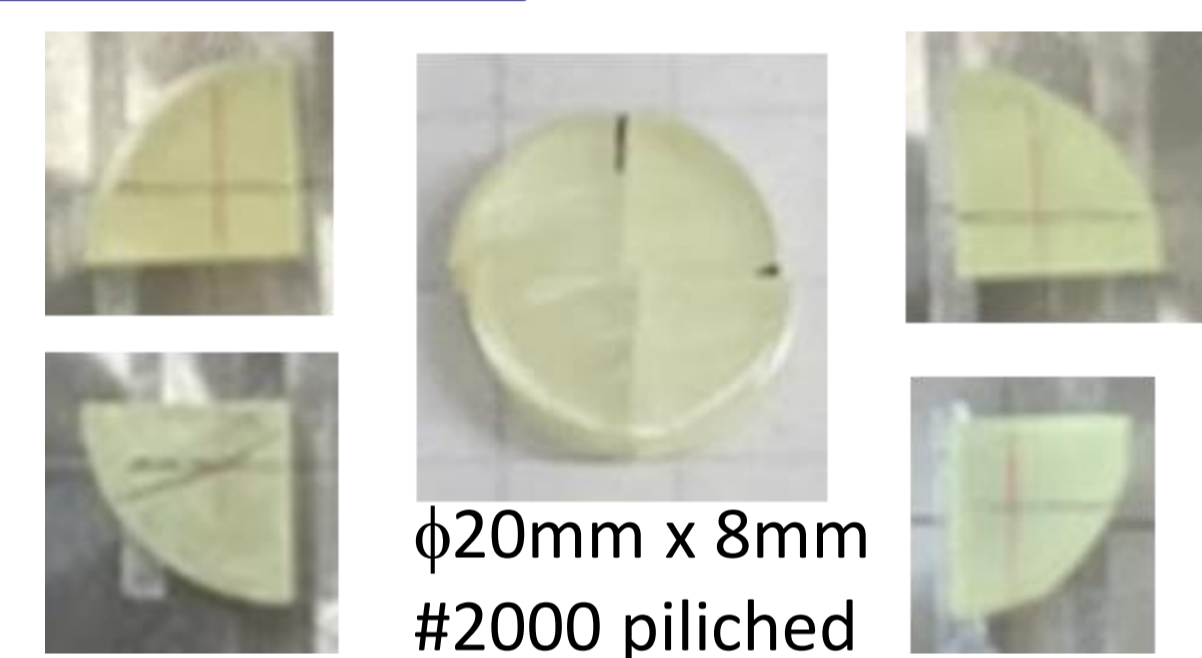
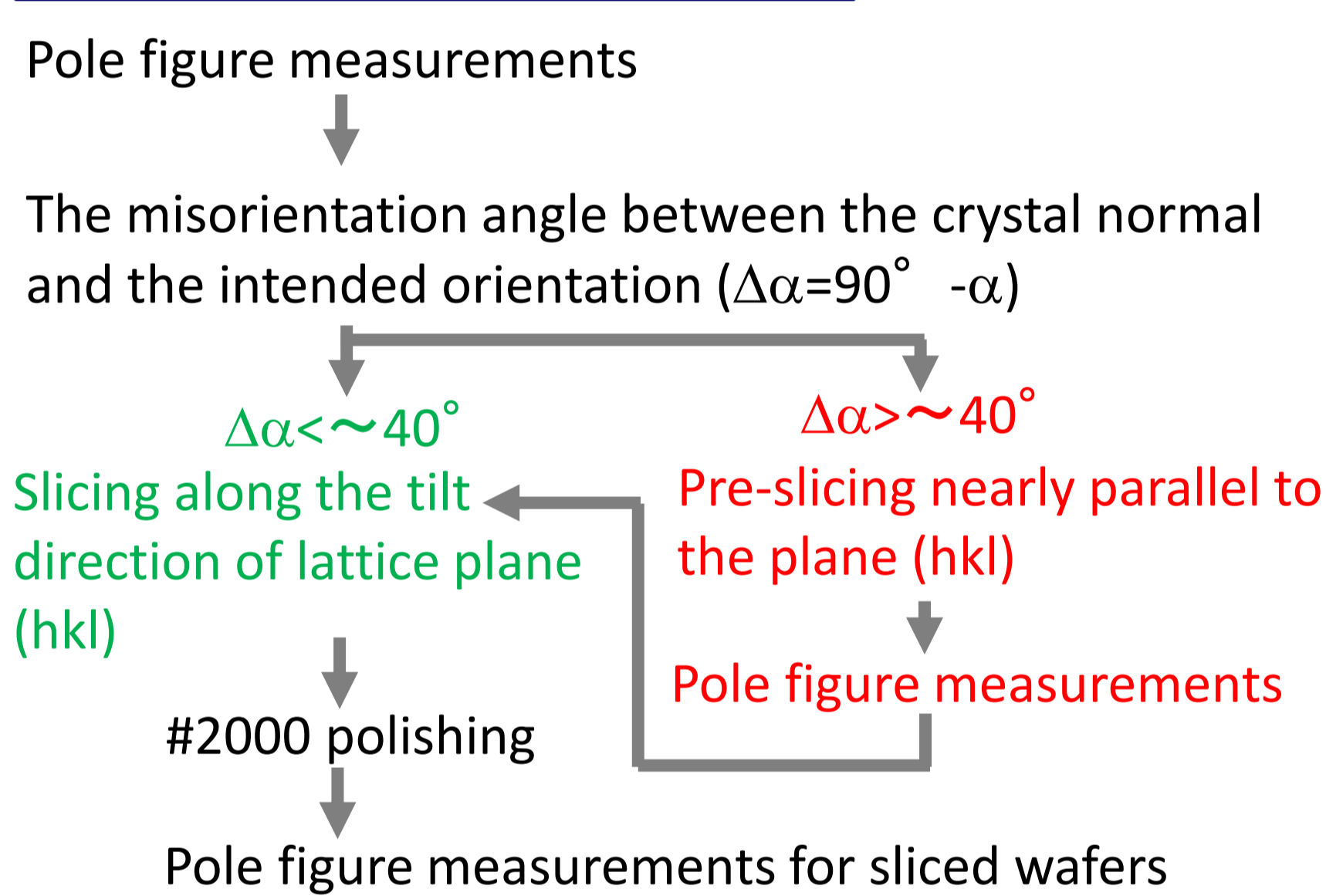


Fig. 4. TlBr crystal (φ20mm x 8mm thick) for pole figure measurements.

Experimental procedure



(100) pole-figure measurements for a starting wafer

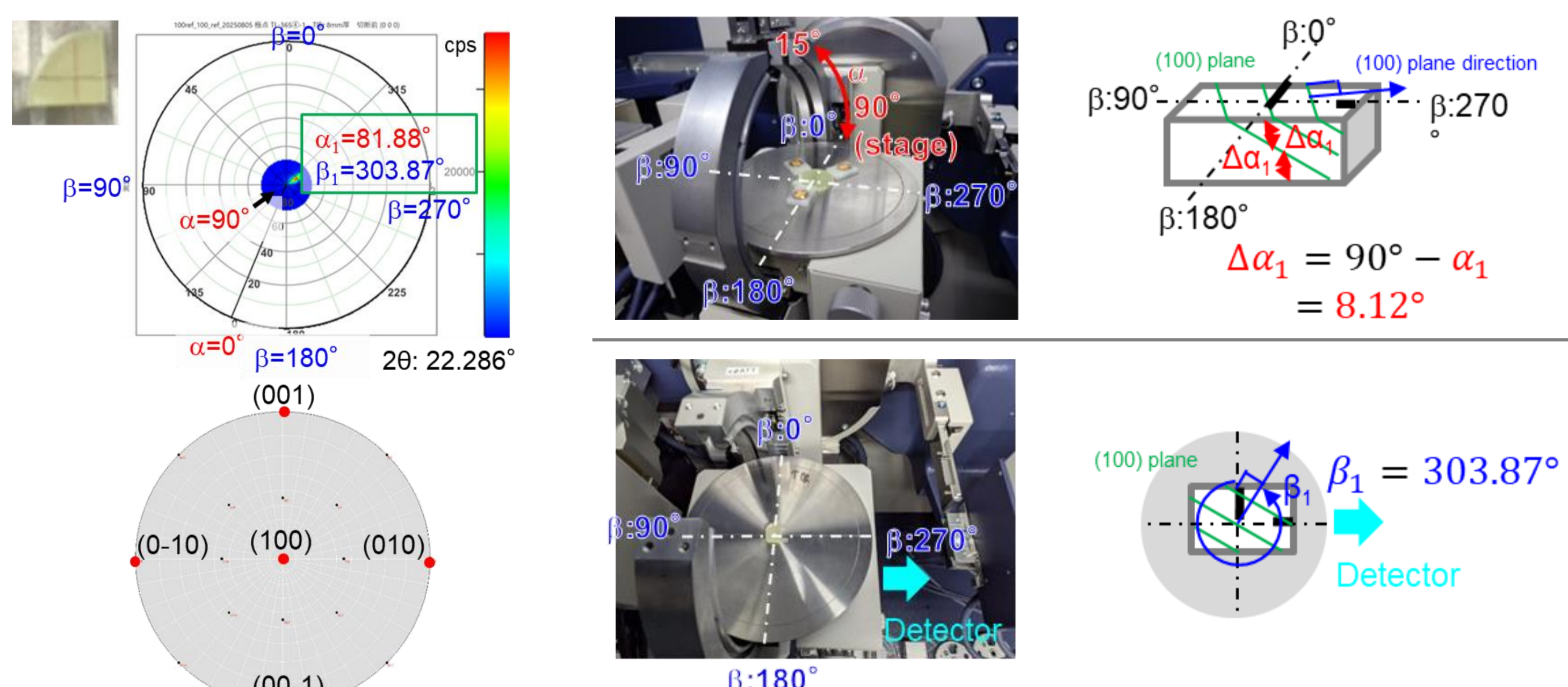


Fig. 5. (100) pole figure of a TlBr wafer and (100) Laue pattern.

Fig. 6. The tilt direction and angle of the (100) plane.

Slicing along (100) plane

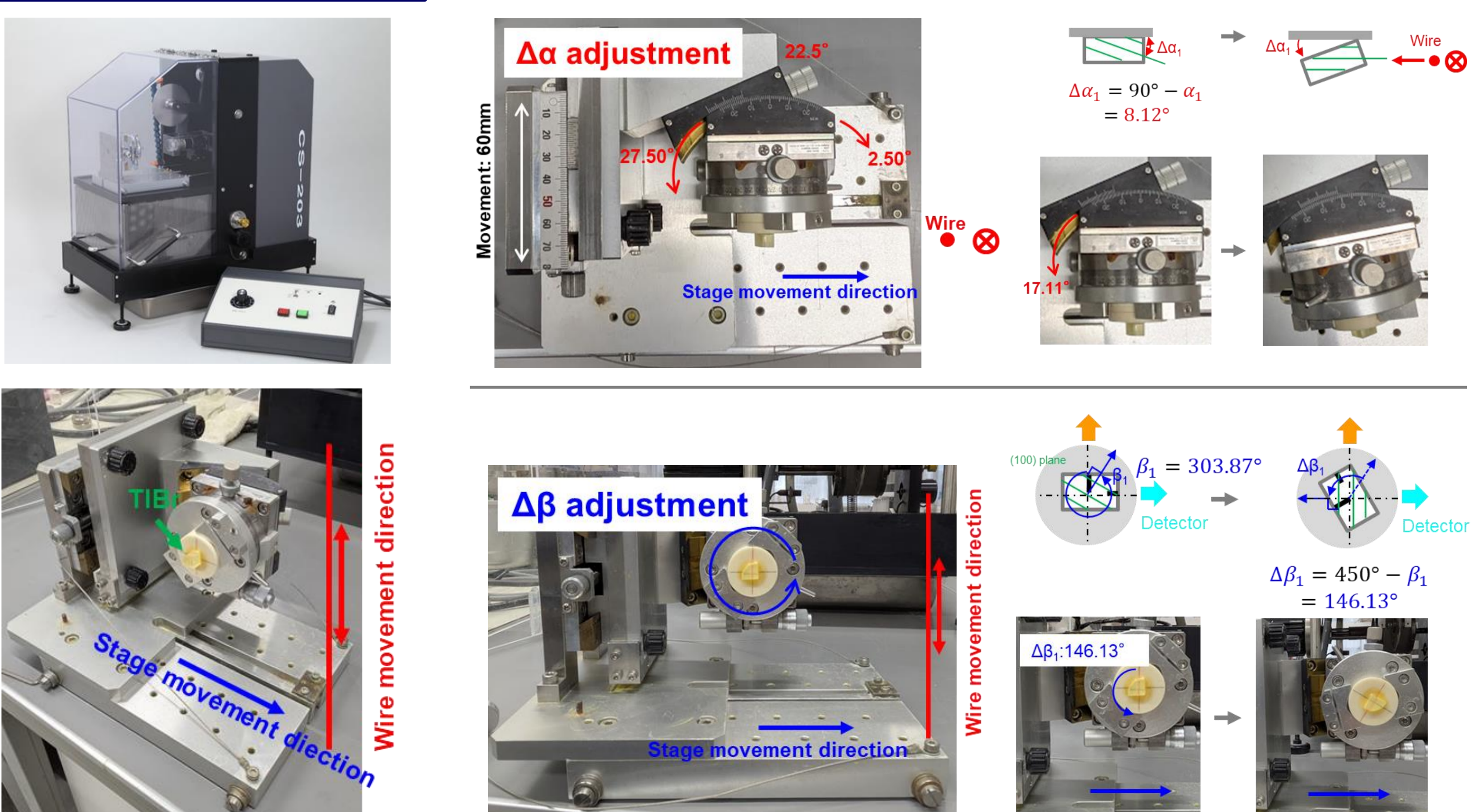


Fig. 7. Diamond wire saw used in this study and the method for adjusting $\Delta\alpha$ and $\Delta\beta$ angle along the (100) plane.

Slicing along (111) plane

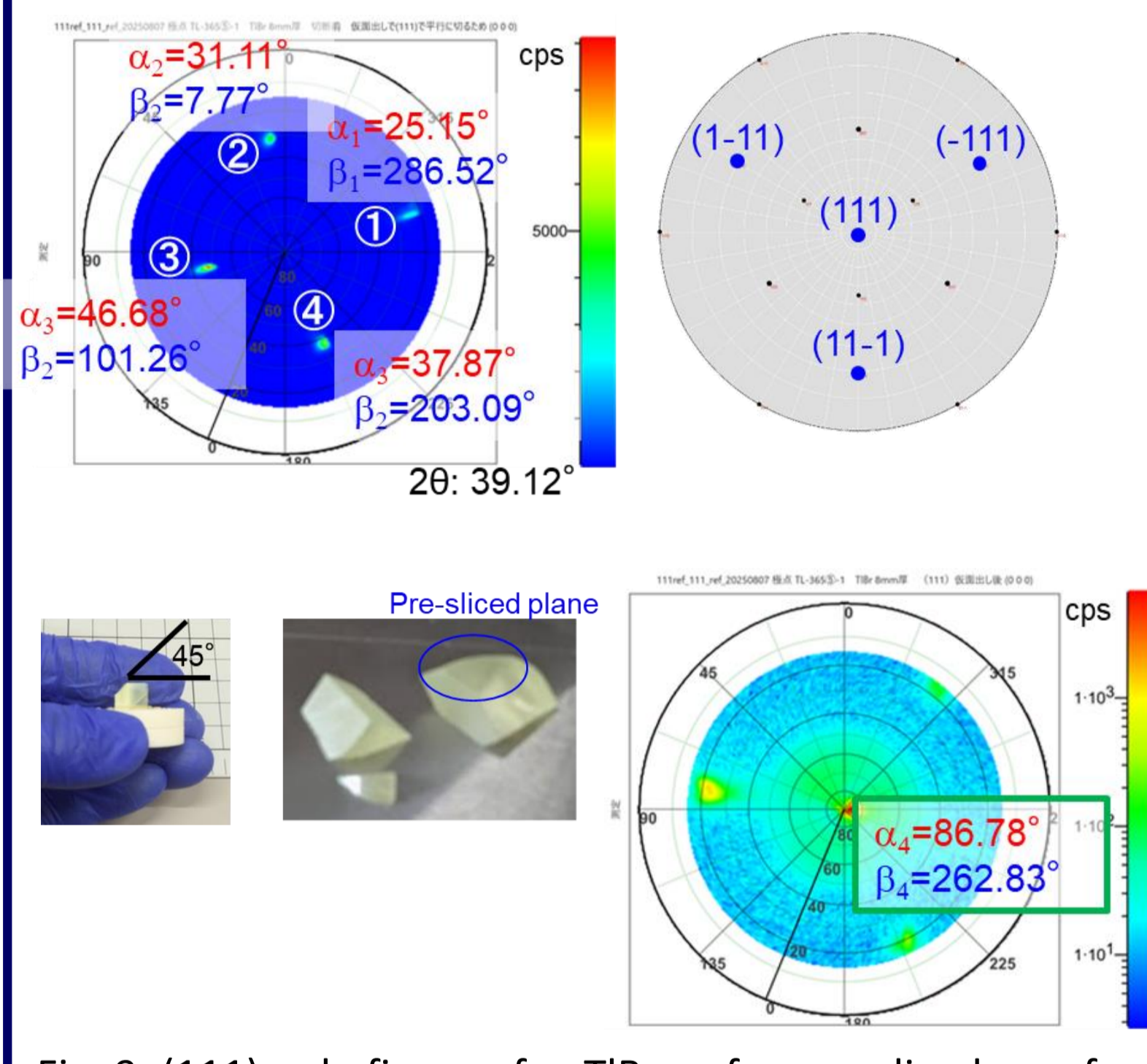
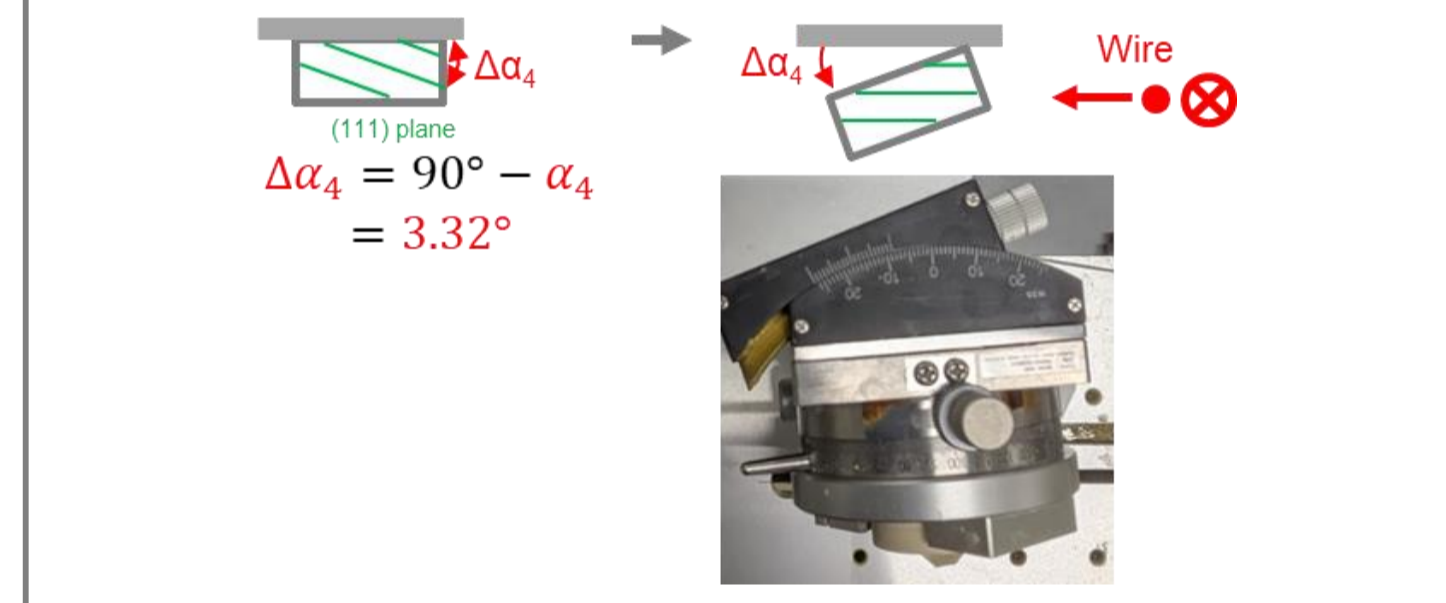


Fig. 9. (111) pole figure of a TlBr wafer, pre-sliced a wafer and (111) Laue pattern.

Δα adjustment



Δβ adjustment

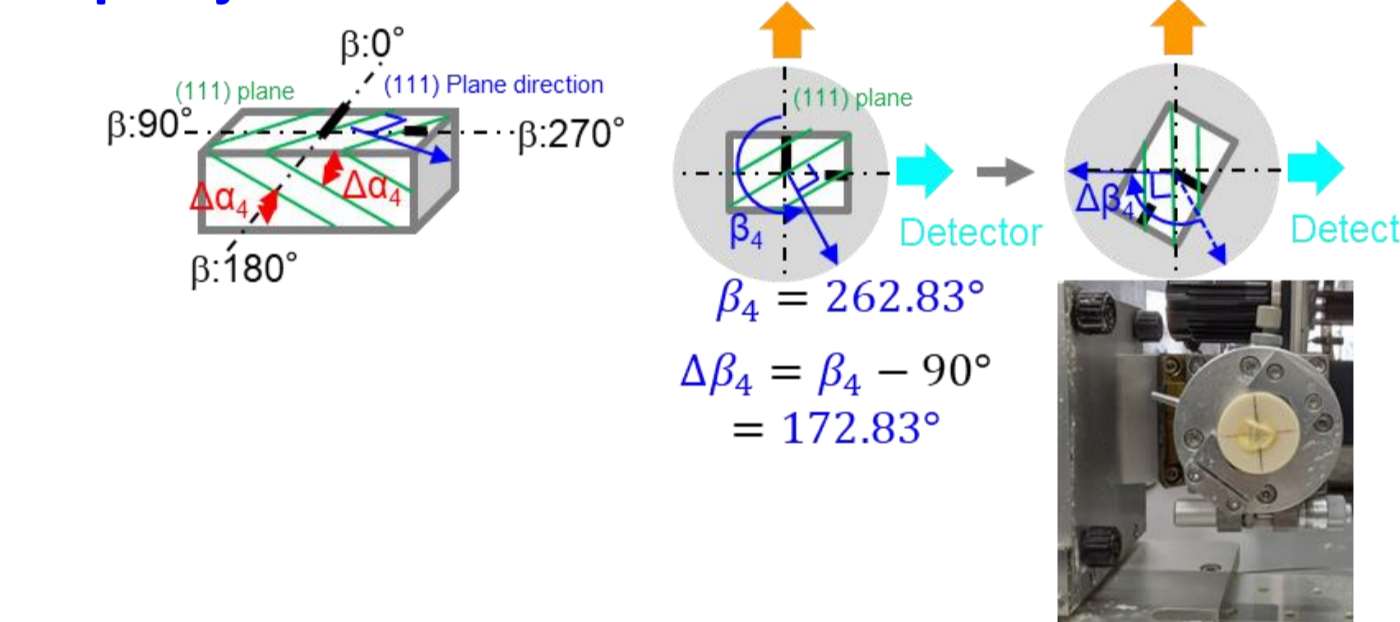


Fig. 10. The method for adjusting $\Delta\alpha$ and $\Delta\beta$ angle along the (111) plane.

Slicing along (110) plane

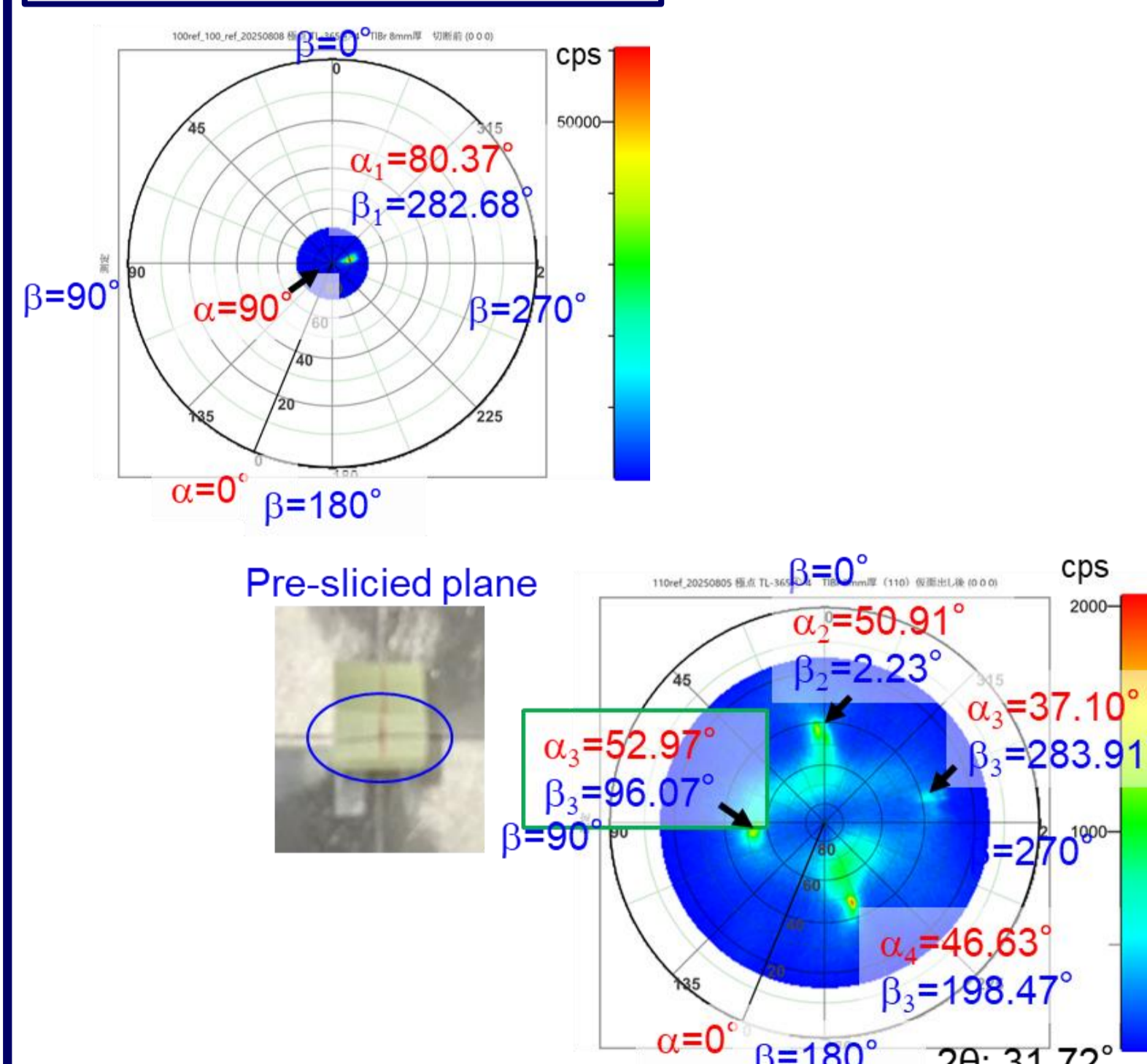
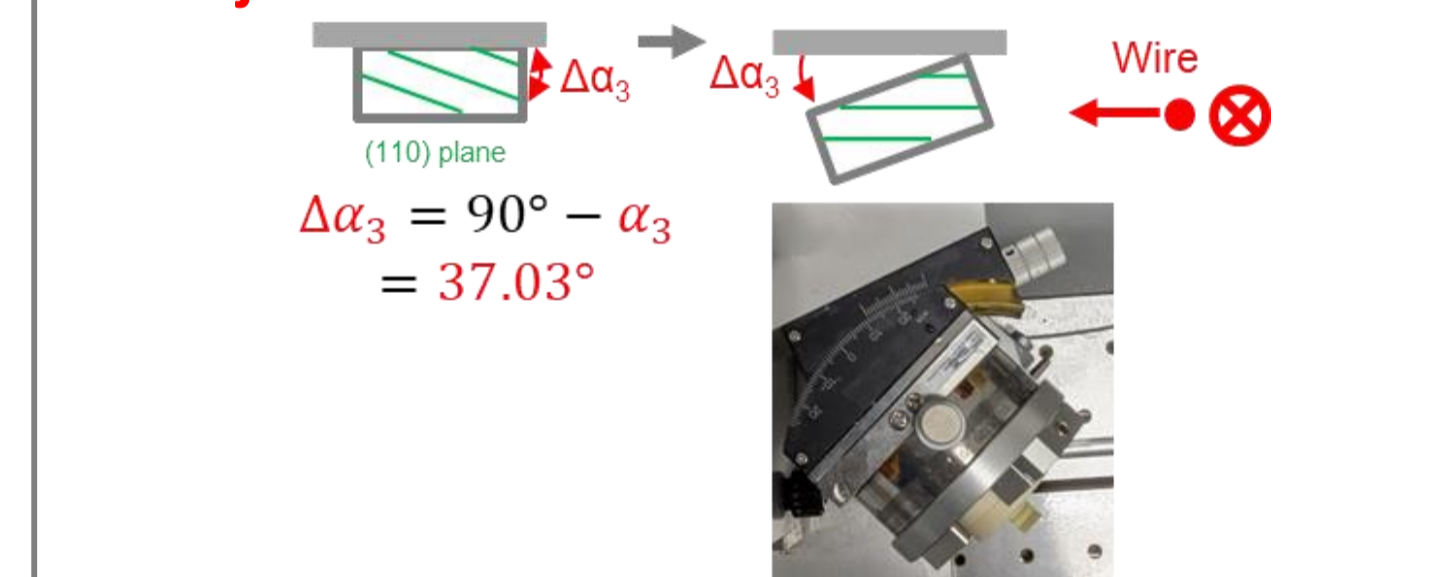


Fig. 11. (110) pole figure of a TlBr wafer, pre-sliced a wafer and (110) Laue pattern.

Δα adjustment



Δβ adjustment

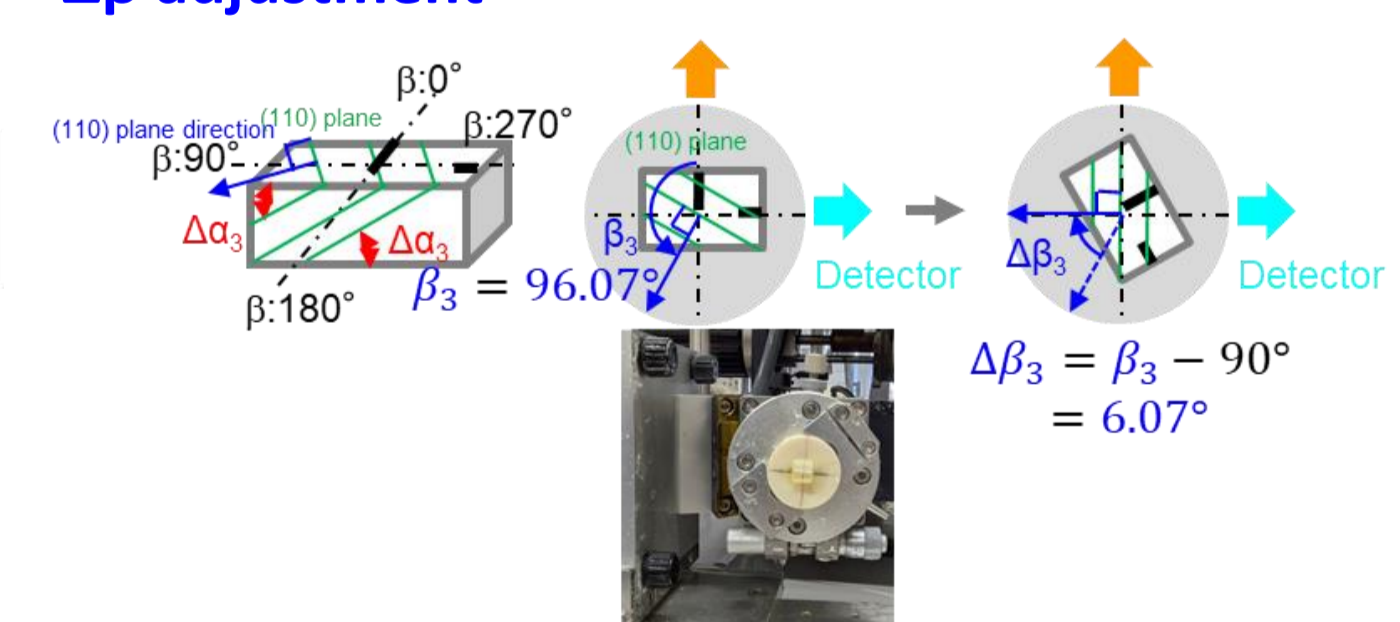


Fig. 12. The method for adjusting $\Delta\alpha$ and $\Delta\beta$ angle along the (110) plane.

Results on orientation cutting

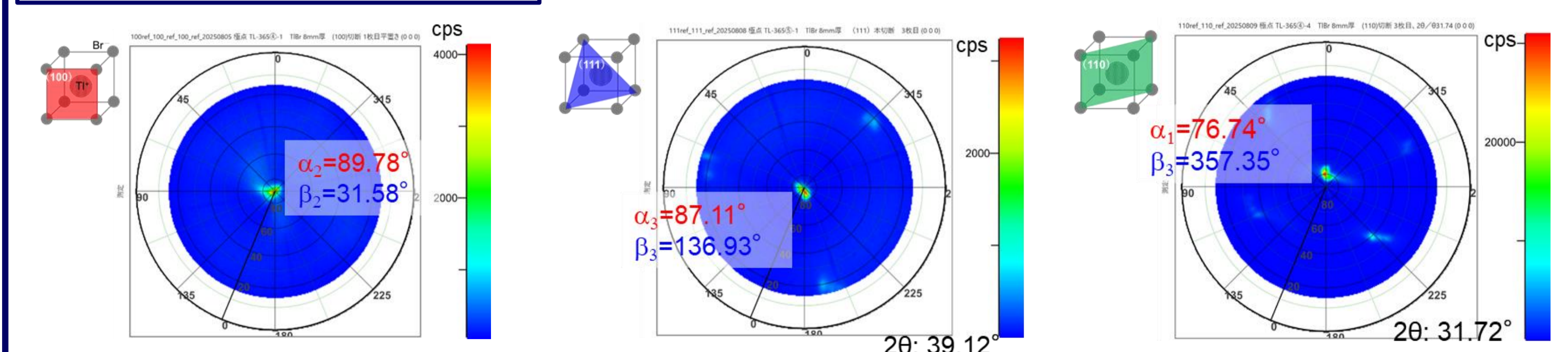


Fig. 12. Pole-figure measurement after the (100), (111) and (110) slicing.

Conclusions

- By using pole-figure measurements and the respective plane orientations, we successfully cut three TlBr wafers with (100), (111) and (110) orientations from a single ingot.
- The deviation from the target orientation is considered to be caused by wire deflection during cutting of the tilted plane.

Acknowledgment: This work was supported by Grant-in-Aid for Scientific Research (A) KAKENHI (24H00230)